



King Saud University  
Arabian Journal of Chemistry

www.ksu.edu.sa  
www.sciencedirect.com



## ORIGINAL ARTICLE

# Precise analysis of thyroxine enantiomers in pharmaceutical formulation by mobility difference based on cyclodextrin



Wanjiao Chen<sup>a</sup>, Weimin Wang<sup>b,\*</sup>, Chuan-Fan Ding<sup>b</sup>, Fangling Wu<sup>b,\*</sup>, Yifeng Mai<sup>a,\*</sup>

<sup>a</sup> Department of Cardiology, the Affiliated Hospital of Medical School, Ningbo University, Ningbo, Zhejiang 315020, China

<sup>b</sup> Zhejiang Provincial Key Laboratory of Advanced Mass Spectrometry and Molecular Analysis, Institute of Mass Spectrometry, School of Material Science and Chemical Engineering, Ningbo University, Ningbo, Zhejiang 315211, China

Received 11 January 2023; accepted 20 February 2023

Available online 25 February 2023

## KEYWORDS

D/L-tetraiodothyronine;  
Separation;  
Ion mobility;  
Chemical theoretical calculations;  
Diastereomer complex;  
Drug tablet

**Abstract** Identification and determination of chiral pharmaceutical residues is still a challenging analytical puzzle. In this work, a simple, rapid, and effective method for chiral D/L-tetraiodothyronine (T4) separation and quantitative was developed based on host–guest recognition using ion mobility spectrometry-mass spectrometry (IMS-MS). The D/L-T4 enantiomers were mobility separated by their diastereomeric complexes through mixing with cyclodextrin (CD) and metal ions. D/L-T4 was first separated by complexing with host molecule ( $\alpha$ -,  $\beta$ -,  $\gamma$ -CD), observing weak peak-to-peak resolution ( $R_{p-p}$ ) by the formed binary complex  $[CD + D/L-T4-H]^+$ , and the  $R_{p-p}$  decreased with the CD size increasing. However, the separation effect of D/L-T4 was much improved with the addition of divalent metal ions ( $G^{2+}$ ) by the formed ternary complex  $[CD + D/L-T4 + G]^{2+}$ . In comparison,  $\alpha$ -CD related complexes can possess the best separation effect for D/L-T4 in most cases. Considering the high selectivity, non-toxic, and chemically stable of  $\beta$ -CD,  $[\beta\text{-CD} + D/L-T4 + Ca]^{2+}$  was selected for D/L-T4 analysis ( $R_{p-p} = 0.764$ ). Whereafter, chemical theoretical conformations for  $[\beta\text{-CD} + D/L-T4 + H]^+$  and  $[\beta\text{-CD} + D/L-T4 + Ca]^{2+}$  were optimized, discovering similar micro-interaction modes between  $[\beta\text{-CD} + D-T4 + H]^+$  and  $[\beta\text{-CD} + L-T4 + H]^+$ ; while with the addition of  $Ca^{2+}$ , significantly different interaction modes were observed between  $[\beta\text{-CD} + D-T4 + Ca]^{2+}$  and  $[\beta\text{-CD} + L-T4 + Ca]^{2+}$ . And theoretical collision cross section (CCS) trends for the complexes were consistent with that of the experimental results. Additionally, calibration curves were linear within  $1.00$  to  $10^4$  ng mL<sup>-1</sup> with coefficient ( $R^2 > 0.99$ ), gaining the limit of detection (LODs) calculation of  $0.11$  ng mL<sup>-1</sup>, and the detection range between D-T4 and L-T4 of  $45.6:1$  to  $1:59.8$ . Finally, the method was applied

\* Corresponding authors.

E-mail addresses: wangweimin1@nbu.edu.cn (W. Wang), wufangling@nbu.edu.cn (F. Wu), fymaiyifeng@nbu.edu.cn (Y. Mai).

Peer review under responsibility of King Saud University.



Production and hosting by Elsevier

for D/L-T4 detection in Levothyroxine tablets, the detection content has good consistency on drug labeling. Because the proposed method exhibited good analytical performance in terms of speed, selectivity, sensitivity, and reproducibility of the measurements, that can be a promising strategy for effective D/L-T4 detection in pharmaceutical industries or other practical samples.

© 2023 The Author(s). Published by Elsevier B.V. on behalf of King Saud University. This is an open access article under the CC BY-NC-ND license (<http://creativecommons.org/licenses/by-nc-nd/4.0/>).

## 1. Introduction

Chiral pharmaceuticals are widely used in different areas of human life, that they may exist in different ecosystems, but the identification and determination of chiral pharmaceutical residues is still a problem and challenge (Dogan et al., 2020). Thyroid hormones (THs) are produced and secreted by the thyroid gland to regulate its metabolism by promoting the physical development, which the THs mainly include triiodothyronine (T3) and tetraiodothyronine (T4) (Luongo et al., 2019). Both excess and deficiency of thyroid hormones can lead to related diseases such as hyperthyroidism, hypothyroidism, thyroid inflammation, goiter, and thyroid cancer (Razvi et al., 2018). T4 has two enantiomeric structures of D-T4 and L-T4, these two enantiomers show different biological and pharmacological activities, among which L-T4 is a synthetic thyroid hormone for the treatment of Hypothyroidism; D-T4 activity is lower than L-T4, generally not used for the treatment of hypothyroidism, besides D-T4 has side effects on the heart that is prohibited for patients with hyperlipidemia (Mourouzis et al., 2011; Cerit et al., 2017). However, many related drugs are used for the treatment of these diseases, such as Thyroid tablets, levothyroxine sodium, liothyronine. Therefore, accurate identification of D-T4 and L-T4 enantiomers in drug synthesis is the premise to ensure the safety use of drugs.

In recently, several methods for T4 enantiomers separation have been reported, such as electro chemiluminescent immunoassay (ECLIA) (Bowerbank et al., 2019), liquid chromatography coupled to a mass spectrometer (Jin et al., 2008; An et al., 2022), electrophoresis (CE) (Woo et al., 2017), and capillary electrochromatography (CEC) (liu et al., 2017). Those methods have their advantages, but also disadvantages were existed. For example, ELISA shows limited sensitivity for THs and these limitations have led to several studies into alternative analytical techniques. As for HPLC, CE, or CEC based method, chiral stationary phase column (CSP) or a chiral mobile phase has the most studies for T4 enantiomer separation, but which also have the drawbacks such as complex chemical derivations, limited and expensive chiral columns, or long-time chromatographic separation.

Mass spectrometry (MS) has attracted increasing attentions for the analysis of THs in recent years, mainly because MS provides mass accuracy, high sensitivity, and has the advantages of fast and simple (Griffiths et al., 2018; Taira et al., 2022; Wu et al., 2022). However, direct analysis of chiral enantiomers by MS is difficult due to the same mass charge ratio. And some works for chiral enantiomers separation by tandem mass spectrum (MS/MS) have been reported, which obtained by comparing the relative intensity difference of their fragment ions (Han et al., 2020; Yu et al., 2017). Undoubtedly, D- and L- pure samples were required, and chemical derivatization with the special chiral selector was also needed in most case.

Ion mobility spectrometry (IMS) is a powerful analytical technique that allows rapid separation of isomeric ions based on differences in mobilities or ion collision cross sections (CCS) in the electric field (Dodds et al., 2019; Putri et al., 2020; Cumeras et al., 2015). The coupling of IMS and MS (IMS-MS) can be an effective technique for isomer separation, as ion mobility adds an extra dimension to the primary MS instrument for separation (Fouque et al., 2019; Wu et al., 2021); Meanwhile, IMS-MS method can overcome the limitation that a single MS cannot separate the ions with the same  $m/z$ ; Otherwise, it enhances the sensitivity of IMS and has  $m/z$  selective analysis characteristics. Trapped ion mobility spectrometry (TIMS), an IMS technique developed by Fernandez-Lima et al. in 2011, uses a  $N_2$  stream to bring

ions into a drift cell and separate them based on size, charge, and shape difference (Fernandez-Lima et al., 2011). And because advantages of simple, quick, high accuracy, the D/L-T4 separation by TIMS-MS based methods are worth studying.

However, it's difficult to achieve the mobility separation of isomers with small structural differences by a single TIMS-MS, especially for chiral enantiomers. However, converting molecules with small structural differences into their diastereomeric complexes with large structural difference, and then realizing their enantiomer separation is effective. Cyclodextrins (CDs) are cyclic oligosaccharide structures formed by the connection of glucose units through (1–4) glycosidic bonds, among which three kinds of CD ( $\alpha$ -,  $\beta$ -,  $\gamma$ -CD) are widely distributed and are used more frequently, and consists of 6, 7 and 8 glucose units, respectively (Ding et al., 2021; Wu et al., 2022). They have numerous and valuable applications in industrial fields such as chemistry, pharmaceutical sciences, food, cosmetics and textiles (Liu et al., 2022). Meanwhile, CDs are often acted as hosts to form complexes with small molecules due to their hydrophilic properties in the inner cavity and hydrophobicity in the outer cavity. Some excellent works about host–guest complexes based on CD have been reported, such as xiao et al. used mercapto- $\beta$ -CD as the host to cap gold nanoclusters as fluorescent probes for succinct and sensitive determination of cholesterol (Xiao et al., 2022); Tang et al. using CD-based host–guest complexes loaded with regorafenib for colorectal cancer treatment (Bai et al., 2021).

In this work, a simple and quick method for D/L-T4 enantiomers separation was developed via complexing with CDs and detecting on TIMS-MS. Specifically,  $\alpha$ -,  $\beta$ -, and  $\gamma$ -CD served as chiral selector to complex with T4 enantiomers, and the enantiomers were analyzed by their formed complexes via TIMS-MS systematically. Subsequently, different bivalent metal ions including  $Mg^{2+}$ ,  $Mn^{2+}$ ,  $Cu^{2+}$ ,  $Ca^{2+}$ ,  $Zn^{2+}$ ,  $Ni^{2+}$ ,  $Fe^{2+}$ ,  $Co^{2+}$ , and  $Ba^{2+}$  were added as ligand to coordinate with T4 and the CDs, to increase the structural difference of the complexes. Meanwhile, chemical theoretical were calculated for the formed complexes to explain the micromolecular interaction and experimental results. Moreover, relative quantitation and absolute quantification for T4 enantiomers was also investigated to validate the stability and reliability of the method. Finally, the method was applied to D-T4 and L-T4 detection in the drugs.

## 2. Experimental section

### 2.1. Chemicals and samples

D-T4 (MW: 776.87, 98%), L-T4 (MW: 776.87, 98%), L-Triiodothyronine (L-T3, MW: 650.97, 98%),  $\alpha$ -CD (MW: 972.84, 98.00%),  $\beta$ -CD (MW: 1134.98, 98.00%), and  $\gamma$ -CD (MW: 1297.12, 98.00%) were obtained from Aladdin Co., Ltd. (Shanghai, China). All inorganic metal salts reported in this work are analytical grade and bought by Shanghai Macklin Biochemical (Shanghai, P. R. China). Methanol (LC-MS grade) and acetonitrile (ACN, LC-MS grade) were acquired from Fisher Scientific Inc. (Pittsburgh, PA). The ESI-Low Concentration Tuning Mix was purchased from Agilent Technologies (Santa Clara, CA). Deionized water used in this work was freshly prepared using a Milli-Q water purification system (Bedford, MA).

## 2.2. Instrumentation and software

All ion mobility analysis for the complexes was performed on a TIMS-TOF instrument from Bruker Daltonik (Bremen, Germany) equipped with electrospray ionization (ESI) source. And the extensive experimental data analysis and processing is performed using the DataAnalysis 5.0 software. And the details are described in the [Supporting Information](#) section 2.

## 2.3. Peak-to-peak resolution

The peak-to-peak resolution ( $R_{p-p}$ ) is used to quantify the degree of separation of the two neighboring peaks, which can be calculated by the following formula: (Wu et al., 2022)

$$R_{p-p} = \frac{2.35 \times (A_2 - A_1)}{(2 \times W_{FWHM1} + 2 \times W_{FWHM2})} \quad (3)$$

Where  $A_1$  and  $A_2$  represent the different  $1/K_0$  of two adjacent peaks, and  $W_{FWHM1}$  and  $W_{FWHM2}$  is their corresponding full peak width at half-maximum.

## 2.4. Chemical calculation

Theoretical structures of the diastereomer complexes of  $[\beta\text{-CD} + \text{D-/L-T4} + \text{H}]^+$  and  $[\beta\text{-CD} + \text{D-/L-T4} + \text{Ca}]^{2+}$  were optimized using the Gaussian program (Weedbrook et al., 2012; Wu et al., 2022). The candidate structures for  $[\beta\text{-CD} + \text{D-/L-T4} + \text{H}]^+$  were first proposed by AutoDock Vina program to get all molecules of interest (Eberhardt et al., 2021), and the preferred structures were further optimized using Gaussian 09 with M062X/LANL2DZ. Besides, the interest structures of  $[\beta\text{-CD} + \text{D-/L-T4} + \text{Ca}]^{2+}$  were measured by AutoDock Vina program via mixing  $\text{Ca}^{2+}$  to the favored structure of  $[\beta\text{-CD} + \text{D-/L-T4} + \text{H}]^+$ . And the favored structures of  $[\beta\text{-CD} + \text{D-/L-T4} + \text{Ca}]^{2+}$  were optimized using Gaussian 09 with M062X/LANL2DZ as well. Vibrational frequencies were calculated to guarantee that the optimized structures corresponded to a stable energy space, and zero-point energy corrections were applied to calculate the relative stability between the structures. Finally, theoretical CCSs for the favored diastereomer complexes were calculated using IMoS software v1.10 (Shrivastav et al., 2017).

## 2.5. Sample pretreatment for the tablet drug

The levothyroxine tablets were bought from the local drug-store in Ningbo (Zhejiang, China), and stored at 4 °C for detection. To extract the analytes, drugs are first removed from the thin film coating and ground to a uniform powder using an agate mortar and pestle. 1.0 g power was dissolved in deionized water (10.0 ml) and sonicated for 2 min. The extract was then filtered by a 0.22  $\mu\text{m}$  drainage filter membrane as the stock solution and stored at 4 °C. The detection solution was obtained by taking 1.0 ml of stock solution and diluted 10-folds with ACN/deionized water (50%:50%, v/v).

## 2.6. Method validation

The proposed method, based on TIMS-MS for D-T4 and L-T4 chiral enantiomer quantitative analysis was validated, which

measured by identifying the different molarities for the isomers (each having ten data points). Relative quantitative were constructed by measuring different isomer mixture ratios, which comprise the molality ratios measured for D-T4: L-T4 ratios range from 10:1 to 1:10 at the concentration level of  $10^{-6}$  mol  $\text{L}^{-1}$ . The mixture was then incubated for 15 min at room temperature to equilibrate before executing the TIMS-MS detection process. Here, the calibration curves of relative quantification for the isomer complexes were constructed by comparing their peak area intensity ratio ( $y$ ) against their corresponding relative concentration ( $x$ ). Moreover, absolute quantification for T4 were also measured by a series of concentrations ranged from 1.00 to  $10^4$  ng  $\text{mL}^{-1}$  containing 10.0 ng  $\text{mL}^{-1}$  of T3 as internal standard, and the calibration curves of absolute quantification was measured on the ratio of the intensities of the mass spectrum peaks (T4/T3). Furthermore, the accuracy of the method was tested by spiking with a known amount of D-T4 and L-T4, which encompassed three different concentrations of a low, medium, and high sensitivity, and was performed in duplicate to determine the average recovery.

## 3. Results and discussion

### 3.1. Mobility separation of T4 enantiomer in complexing with CDs

The MS and mobility analyses were first performed for the T4 enantiomers by complexing with CDs. As shown in Fig. 2, the  $m/z$  777.00, 1750.02, 1912.08, and 2074.15 are contributed to the ions of  $[\text{T4} + \text{H}]^+$ ,  $[\alpha\text{-CD} + \text{T4} + \text{H}]^+$ ,  $[\beta\text{-CD} + \text{T4-H}]^+$ , and  $[\gamma\text{-CD} + \text{T4-H}]^+$ , respectively. The results revealed that the T4 enantiomers can non-covalent interaction with CDs and form the corresponding binary complex of  $[\text{TH} + \text{CD-H}]^+$ . And then their mobility analysis was studied. As shown in Fig. 1, the identical extraction ion mobilities (EIMs) were found for the complexes of  $[\text{D-T4} + \text{H}]^+$  and  $[\text{L-T4} + \text{H}]^+$ , revealing that the D and L-T4 enantiomers cannot be mobility separated by their own protonated ions.

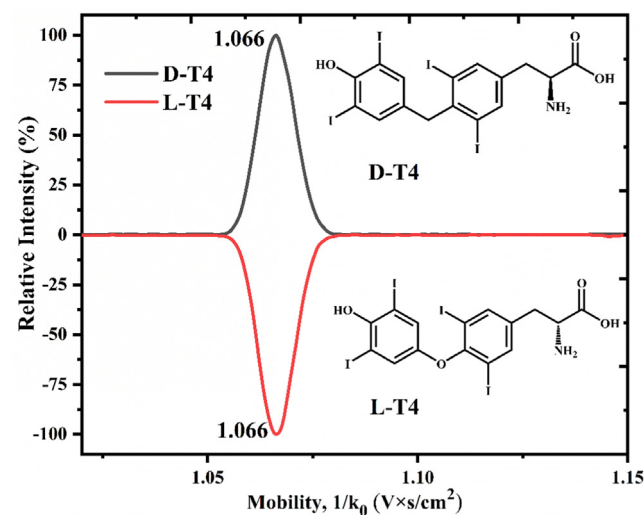


**Fig. 1** The extracted ion mobility spectra and structure for the D/L-T4 enantiomers.

Besides, TIMS analysis for the binary complexes of  $[\text{CD} + \text{T4-H}]^+$  were studied and shown in the right of Fig. 2. The EIMs between the  $[\text{CD} + \text{D-T4-H}]^+$  and  $[\text{CD} + \text{L-T4} + \text{H}]^+$  have certain difference. Specifically, the mobility value for  $[\alpha\text{-CD} + \text{D-T4} + \text{H}]^+$  is  $1.767 \text{ V}\cdot\text{s}\cdot\text{cm}^{-2}$  and for  $[\alpha\text{-CD} + \text{D-T4} + \text{H}]^+$  is  $1.774 \text{ V}\cdot\text{s}\cdot\text{cm}^{-2}$ , which the calculated  $R_{p-p}$  is 0.411. Identical, the mobility value for  $[\beta\text{-CD} + \text{D/L-T4} + \text{H}]^+$  and  $[\gamma\text{-CD} + \text{D/L-T4} + \text{H}]^+$  are 1.754/1.758 and 1.847/1.849  $\text{V}\cdot\text{s}\cdot\text{cm}^{-2}$ , with the  $R_{p-p}$  for D/L-T4 separation are 0.235 and 0.118, respectively. The results reveal that the separation effect  $R_{p-p}$  for D/L-T4 enantiomer was decreased as the size of the inner cavity of the CD increasing, which probably because the large CD inner cavity allows more entry of the target analyte that resulting in less structural difference for the diastereomer complex.

### 3.2. Mobility separation of T4 in complexing with CDs and metal ions

Through the D/L-T4 enantiomer can be mobility recognized by their formed binary complexes, but the resolution is not sat-

isfactory when their enantiomeric complexes coexist. In this case, the center ligand of metal ions was added to study their separation effect. As shown in the left of Fig. 3,  $\text{Ca}^{2+}$  was served as an example to complex with the CDs and the D/L-T4, which  $m/z$  894.83, 975.52, 1056.55 are attributed to the complex ions of  $[\alpha\text{-CD} + \text{T4} + \text{Ca}]^{2+}$ ,  $[\beta\text{-CD} + \text{T4} + \text{Ca}]^{2+}$ , and  $[\gamma\text{-CD} + \text{T4} + \text{Ca}]^{2+}$ , respectively. The MS results reveal that  $\text{Ca}^{2+}$  can as a ligand to coordinate with CD and T4, and the corresponding ternary complexes can be formed. For other MS peaks in the mass spectra, which are the complexes formed by the interaction of CD with other substances, because metal salts are only in analytical grade and the contaminants may be present in the mass spectrometer. And then the mobility study was measured for the ternary complexes. As shown in the right of Fig. 3, significantly different EIMs were observed for the D- and L-ternary complexes. For example, mobility values for  $[\alpha\text{-CD} + \text{D-T4} + \text{Ca}]^{2+}$  and  $[\alpha\text{-CD} + \text{L-T4} + \text{Ca}]^{2+}$  are 0.941 and 0.951  $\text{V}\cdot\text{s}\cdot\text{cm}^{-2}$ , with the calculated  $R_{p-p}$  of 0.529. Similarly, mobility values for  $[\beta\text{-CD} + \text{D/L-T4} + \text{Ca}]^{2+}$  and  $[\gamma\text{-CD} + \text{D/L-T4} + \text{Ca}]^{2+}$  are 0.967/0.981 and 1.015/1.023  $\text{V}\cdot\text{s}\cdot\text{cm}^{-2}$ , resulting in  $R_{p-p}$  of 0.764 and 0.470, respectively.

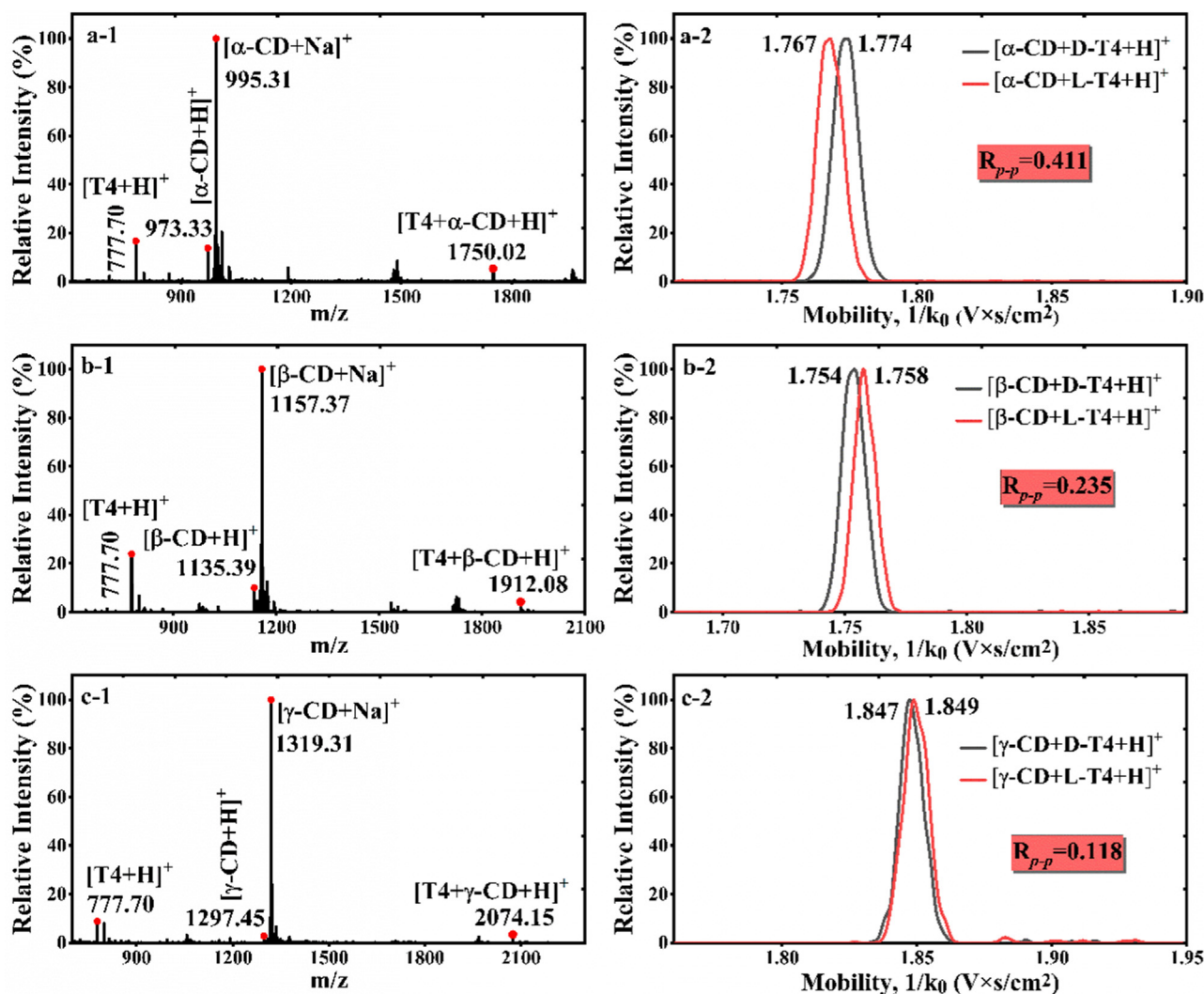
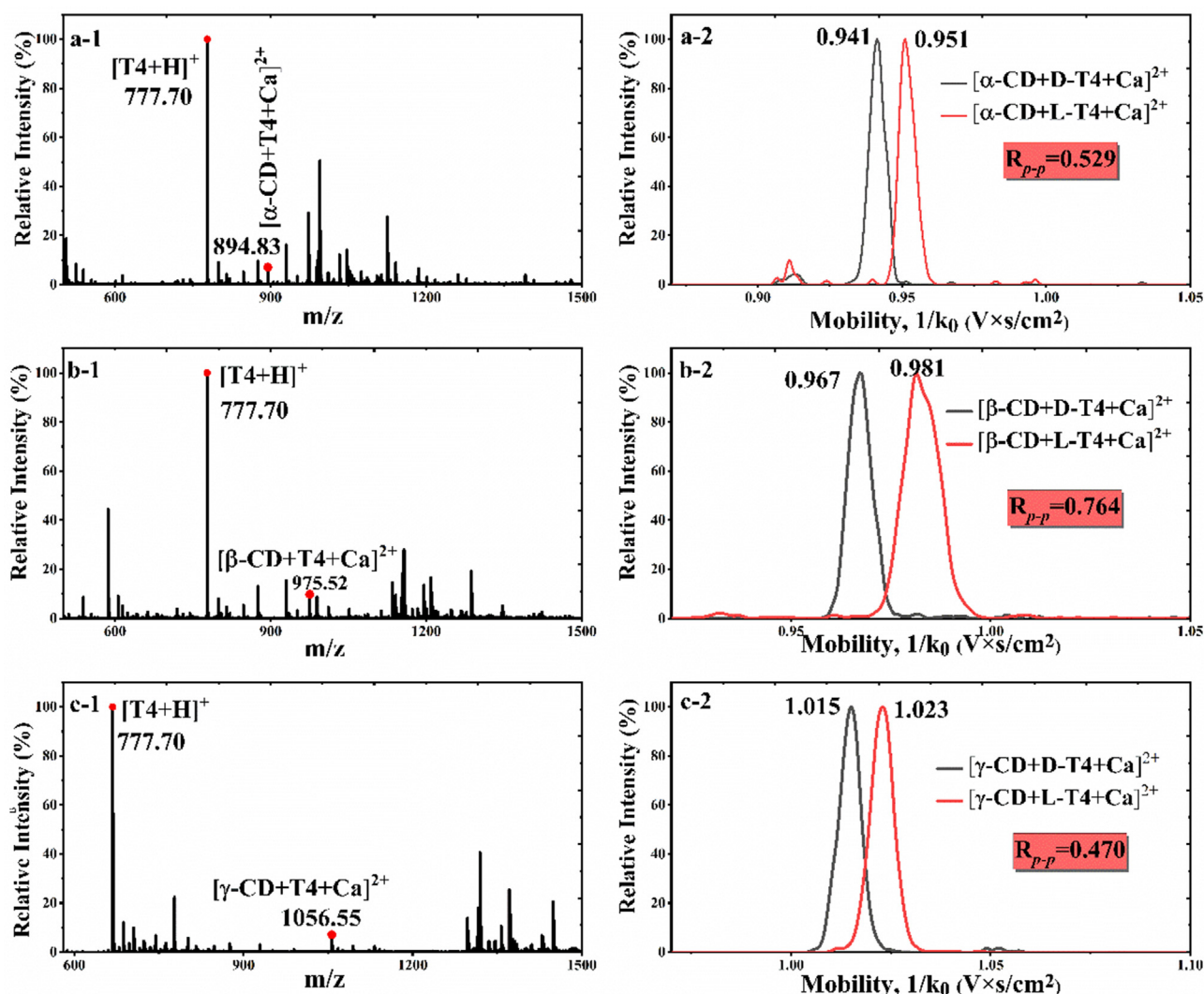


Fig. 2 Mass spectra for TH in complex with CDs and their corresponding EIM (a)  $[\alpha\text{-CD} + \text{T4} + \text{H}]^+$ ; (b)  $[\beta\text{-CD} + \text{T4} + \text{H}]^+$ ; (c)  $[\gamma\text{-CD} + \text{T4} + \text{H}]^+$ .





**Fig. 3** Mass spectra for TH in complex with CDs and  $\text{Ca}^{2+}$  and their corresponding extracted ion mobility (a)  $[\alpha\text{-CD} + \text{T4} + \text{Ca}]^{2+}$ ; (b)  $[\beta\text{-CD} + \text{T4} + \text{Ca}]^{2+}$ ; (c)  $[\gamma\text{-CD} + \text{T4} + \text{Ca}]^{2+}$ .

In addition, other divalent metal ions of  $\text{Mg}^{2+}$ ,  $\text{Mn}^{2+}$ ,  $\text{Fe}^{2+}$ ,  $\text{Co}^{2+}$ , and  $\text{Ni}^{2+}$  were also studied as ligand for D/L-T4 separation. As shown in Fig. 4, the studied metal ions all have different effect for D/L-T4 separation, which the  $R_{p-p}$  can reach to 1.59 by the formed complex of  $[\alpha\text{-CD} + \text{D/L-T4} + \text{Ni}]^{2+}$ . In comparison,  $\alpha\text{-CD}$  related complex seems has the best separation effect for D/L-T4 enantiomers in most case. However, the separation resolution of the D/L-T4 may be reduced with the coordinated of the metal ions ( $\text{Mn}^{2+}$ ), which probably because  $\text{Mn}^{2+}$  was interact with the narrow rim of the CD, and majority of the D/L-T4 is in the CD chamber, that reduced their separation effect and have essentially the same separation resolution. But this is not the focus of this work just an empirical guess, and the specific results require further theoretical calculations. And the accuracy for the method was measured in quintuplicate in consecutive days, the calculated RSD% was in a range of 0.22 to 0.50 %, revealing the method has good repeatability and stability. Moreover, considering D/L-T4 can be baseline separation by complexing with  $\beta\text{-CD}$  and  $\text{Ca}^{2+}$  ( $R_{p-p} = 0.764$ ) (Fig. 3b-2), and the

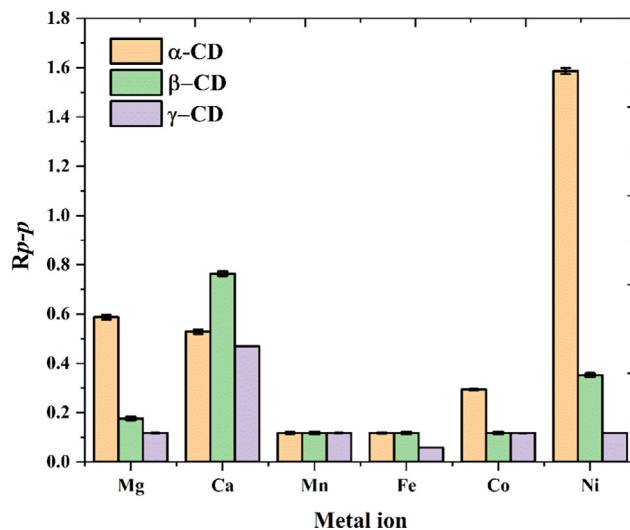


**Fig. 4** Separation effect  $R_{p-p}$  for the D/L-T4 by complex with different metal ions and CDs.

advantages of high selectivity, non-toxic, chemically stable of  $\beta$ -CD, that  $[\beta\text{-CD} + \text{D/L-T4} + \text{Ca}]^{2+}$  was selected for further studying.

### 3.3. Parameter optimization for detection

Detection parameters such as solvent, molar ratio among CD, metal salts and T4, and ionization voltage all can affect the formation of the complexes. In this case, the formation of  $[\beta\text{-CD} + \text{D/L-T4} + \text{Ca}]^{2+}$  was studied. As shown in Fig. 5a and Fig. 5b, methanol and ACN as solvent were investigated, revealing ACN was more benefited for the formation of  $[\beta\text{-CD} + \text{D/L-T4} + \text{Ca}]^{2+}$  than methanol. Besides, the relative intensity of the complex was increased when ACN content was increased from 30% to 50%, and when ACN content continued to increase, its intensity decreased. More-

over, the molar ratio among the  $\beta$ -CD, T4 and  $\text{Ca}^{2+}$  was studied, with the molar ratio of  $\text{Ca}^{2+}$  to T4 increased from 0.4 to 0.8, the relative intensity of  $[\beta\text{-CD} + \text{D/L-T4} + \text{Ca}]^{2+}$  was increasing, but its intensity of the complexes was decreased as the molar concentration of the salt was continued to increase (Fig. 5c). Similarly, the molar ratio of  $\beta$ -CD to T4 was also studied, a molar ratio of 1.0:0.8:0.8 for T4:  $\beta$ -CD:  $\text{Ca}^{2+}$  was best (Fig. 5d). The flow rate was further optimized, it was shown that the strength of the complex decreases with the increase of the flow rate (Fig. 5e). Finally, the ionization voltage was optimized in Fig. 5f, as the ionization voltage increase, the detection efficiency of the target decreases instead, revealing that 3000 V is the favored ionization efficiency in this case. Thus, the favored detection parameters were as follows, the molar ratio of T4:  $\beta$ -CD:  $\text{Ca}^{2+}$  was 1.0:1.2:0.8, solvent was 50% ACN /water, detection flow rate was  $2 \text{ ul min}^{-1}$ , and the ionization voltage was 3000 V.

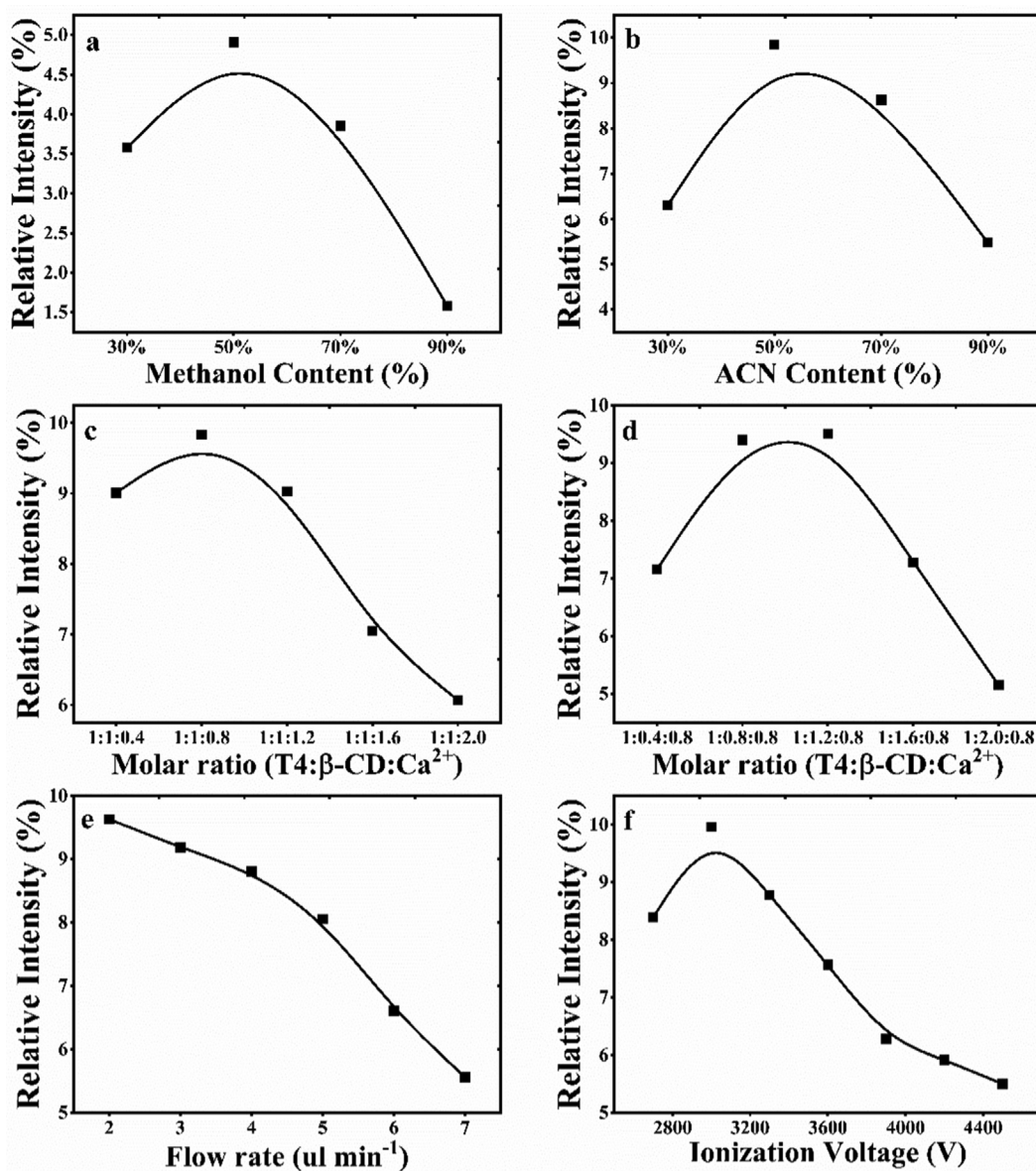


**Fig. 5** Parameter optimization for the detection of complex  $[\beta\text{-CD} + \text{T4} + \text{Ca}]^{2+}$  (a) Methanol content in the solvent; (b) ACN content in the solvent; (c) Molar ratio of  $\text{Ca}^{2+}$  to T4; (d) Molar ratio of  $\beta$ -CD to T4; (e) flow rate of detection; (f) ionization voltage;

### 3.4. Chemical theoretical calculation

The mobility differences of the diastereomeric complexes revealed D/L-T4 have different interaction effects with the CDs. The favored conformation for the complexes were optimized to match and explain their micro-interactions (Campuzano, et al., 2012; Shrivastav, et al., 2017). The possible structures for each complex were first optimized by Auto-Dock software, and the structures with low energy were selected and further optimized to obtain the final structure by Gaussian. Herein, the favored conformations of D/L-T4 in complexing with  $\beta$ -CD and  $\text{Ca}^{2+}$  were optimized as examples for interpretation by chemical theoretical calculations using M062X/LANL2DZ (Detailed in the [Supporting Information](#)), and the energy for the complexes are shown in [Table S1](#) and [Table S2](#). As showed in [Fig. 6a](#) and [Fig. 6b](#), similar modes of interaction were observed for  $[\beta\text{-CD} + \text{D-T4} + \text{H}]^+$  and  $[\beta\text{-CD} + \text{L-T4} + \text{H}]^+$ . The CCS values between experimental and chemical theoretical for the complexes were displayed in [Table 1](#), theoretical CCSs for  $[\beta\text{-CD} + \text{D-T4} + \text{H}]^+$  and  $[\beta\text{-CD} + \text{L-T4} + \text{H}]^+$  are 387.63 and 383.56  $\text{\AA}^2$ , which have good consistent trend with the experimental values. Meanwhile, the structural difference for the complexes was expanded with the addition of  $\text{Ca}^{2+}$ . As shown in [Fig. 6c](#) and [Fig. 6d](#),  $\text{Ca}^{2+}$  interacts with  $\beta$ -CD and D/L-T4 at different locations, where  $\text{Ca}^{2+}$  wrapped inside D-T4 and  $\beta$ -CD, while  $\text{Ca}^{2+}$  was interact with T4 on the small orifice surface of  $\beta$ -CD. Accordingly, the theoretical CCSs for  $[\beta\text{-CD} + \text{D-T4} + \text{Ca}]^{2+}$  and  $[\beta\text{-CD} + \text{L-T4} + \text{Ca}]^{2+}$  are 440.03 and 431.65  $\text{\AA}^2$ , compared with their experimental CCSs values of 399.0 and 392.0  $\text{\AA}^2$  ([Table 1](#)), similar trend of the CCS value changes ( $\text{RSD} \leq 13.87\%$ ) were obtained.

**Table 1** CCS measurement for  $[\beta\text{-CD} + \text{T4} + \text{H}]^+$  and  $[\beta\text{-CD} + \text{T4} + \text{Ca}]^{2+}$  by experimental and theoretical.

Complex	TIMS (CCS $\text{\AA}^2$ )	DFT (CCS $\text{\AA}^2$ )	RSD (%)
$[\beta\text{-CD} + \text{D-T4} + \text{H}]^+$	340.4	387.63	13.87
$[\beta\text{-CD} + \text{L-T4} + \text{H}]^+$	338.3	383.56	13.38
$[\beta\text{-CD} + \text{D-T4} + \text{Ca}]^{2+}$	399.0	440.03	10.28
$[\beta\text{-CD} + \text{L-T4} + \text{Ca}]^{2+}$	392.0	431.65	10.11

Indeed, CCS value errors between the experimental and theoretical were between 10.11 and 13.87%, which were caused by the structural form difference between the calibrated tuning mixture and the diastereomer complexes, the trajectory method for CCS calculation, and the parameter setting of the IMoS program. However, the CCS trends are consistent between experiment and theory (Olajide et al., 2021), the conformation difference for D-/L-T4 was increased by interaction with  $\beta$ -CD and  $\text{Ca}^{2+}$  and resulted in different effects on the mobility separation.

### 3.5. Quantitative analysis for the D/L-T4 enantiomers

As the D/L-T4 can be separated by the proposed method, that their quantitative analysis of absolute and relative quantification was evaluated. Herein, the absolute quantitative was measured with L-T3 as the internal standard, keeping L-T3 in a fixed concentration ( $10.00 \text{ ng mL}^{-1}$ ), and changing the concen-

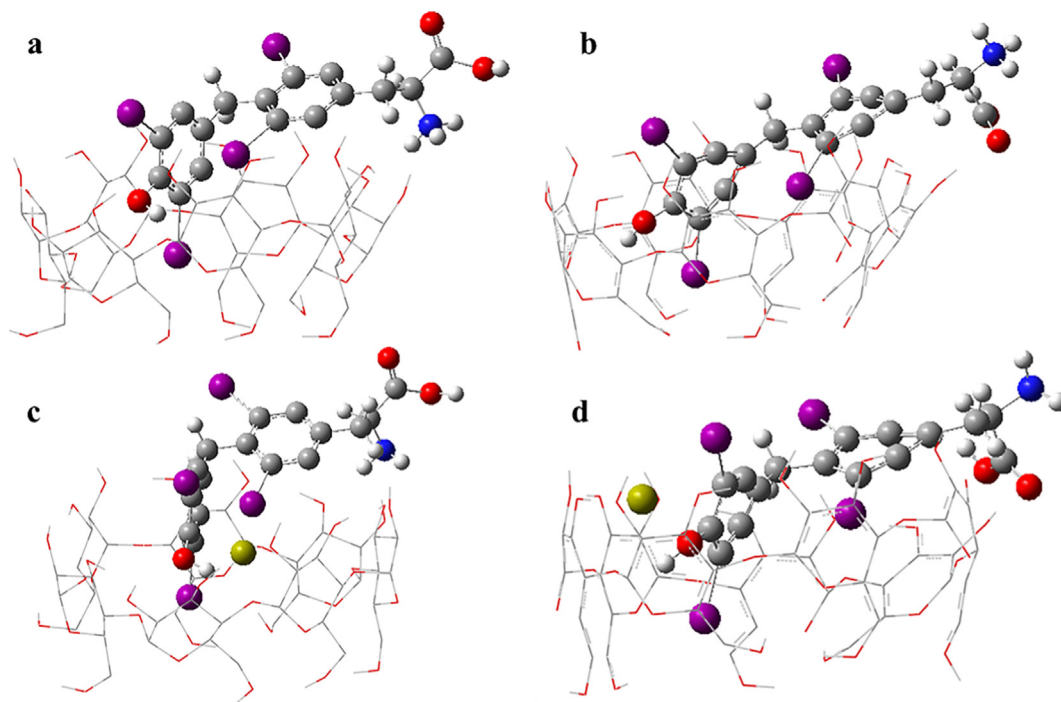


**Fig. 6** Structure for the complexes of (a)  $[\beta\text{-CD} + \text{D-T4} + \text{H}]^+$ ; (b)  $[\beta\text{-CD} + \text{L-T4} + \text{H}]^+$ ; (c)  $[\beta\text{-CD} + \text{D-T4} + \text{Ca}]^{2+}$ ; (d)  $[\beta\text{-CD} + \text{L-T4} + \text{Ca}]^{2+}$ .



tration of D/L-T4 from 1.00 to  $10^4$  ng mL<sup>-1</sup> in seven points. As shown in Fig. 7a, MS spectra of mixtures of L-T3 (10.00 ng mL<sup>-1</sup>), D/L-T4 (1:1, 50.0 ng mL<sup>-1</sup>), and Na<sup>+</sup> (100.0 ng mL<sup>-1</sup>) were studied, the ions were present as the form of Na<sup>+</sup> coordination, such as the ions of [T4/T3 + Na]<sup>+</sup>, [T4/T3 + 2Na-H]<sup>+</sup>, [T4/T3 + 3Na-2H]<sup>+</sup>. In this case, the absolute quantitative was measured by the intention of [T4 + H]<sup>+</sup>, [T4 + Na]<sup>+</sup>, [T4 + 2Na-H]<sup>+</sup>, [T4 + 3Na-2H]<sup>+</sup> to the intensity of [L-T3 + H]<sup>+</sup>, [L-T3 + Na]<sup>+</sup>, [L-T3 + 2Na-H]<sup>+</sup>, [L-T3 + 3Na-2H]<sup>+</sup>. The results are shown in Fig. 7b, yielding good linear ( $R^2 = 0.9904$ ) with an RSD slope of 1.26% ( $n = 5$ ); the limit of detection (LODs) and limit of quantitation (LOQ) calculation for the T4 by the signal-to-noise ratio ( $S/N = 3$ ) and ( $S/N = 10$ ) were 0.11 ng mL<sup>-1</sup> and 0.49 ng mL<sup>-1</sup>, respectively.

Besides, a series of different molar ratios of D-T4 and L-T4 changed from 10:1 to 1:10 in complexing with  $\beta$ -CD and Ca<sup>2+</sup> were measured. EIMs for the diastereomer complexes [ $\beta$ -CD + T4 + Ca]<sup>2+</sup> obtained by the mixtures are shown in Fig. 7c, the mobility intensity for the ions was increased with its ratios increasing. And the calibration curve for D/L-T4 relative quantification was assessed by plotting the mobility peak area intensity of D-T4/L-T4 versus the relative concentration

of D-T4/L-T4. As displayed in Fig. 7d, good linear relationship between the relative intensity and the relative concentration with a  $R^2$  value of 0.9901, and RSD ( $n = 5$ ) of 2.78% were obtained. Moreover, the detection scope of the method was also measured, which in the range of 45.6:1 to 1:59.8 by the proposed method.

Moreover, accuracy of quantitative analysis by the method was further measured by quality control (QC) in three different concentrations and back-calculation using the calibration curves. For the accuracy of absolute quantification, QC in three concentrations of low (3.0 ng mL<sup>-1</sup>), medium (500.0 ng mL<sup>-1</sup>) and high (9000.0 ng mL<sup>-1</sup>), and three molar ratios for relative quantification were low (10:3), medium (10:9), and high (1:9) were measured. The detection results are shown in Table 2, accept accuracy with  $RSD \leq 5.67\%$ . And a simple comparison of the proposed method with the prior methods was measured in Table S3, this method has the advantages of high sensitivity, short time and simple operation. Thus, the relative quantification results revealed that the proposed method based on complexing with  $\beta$ -CD and Ca<sup>2+</sup> and detected on TIMS-MS, can be a promising approach for D/L-T4 enantiomer detection.

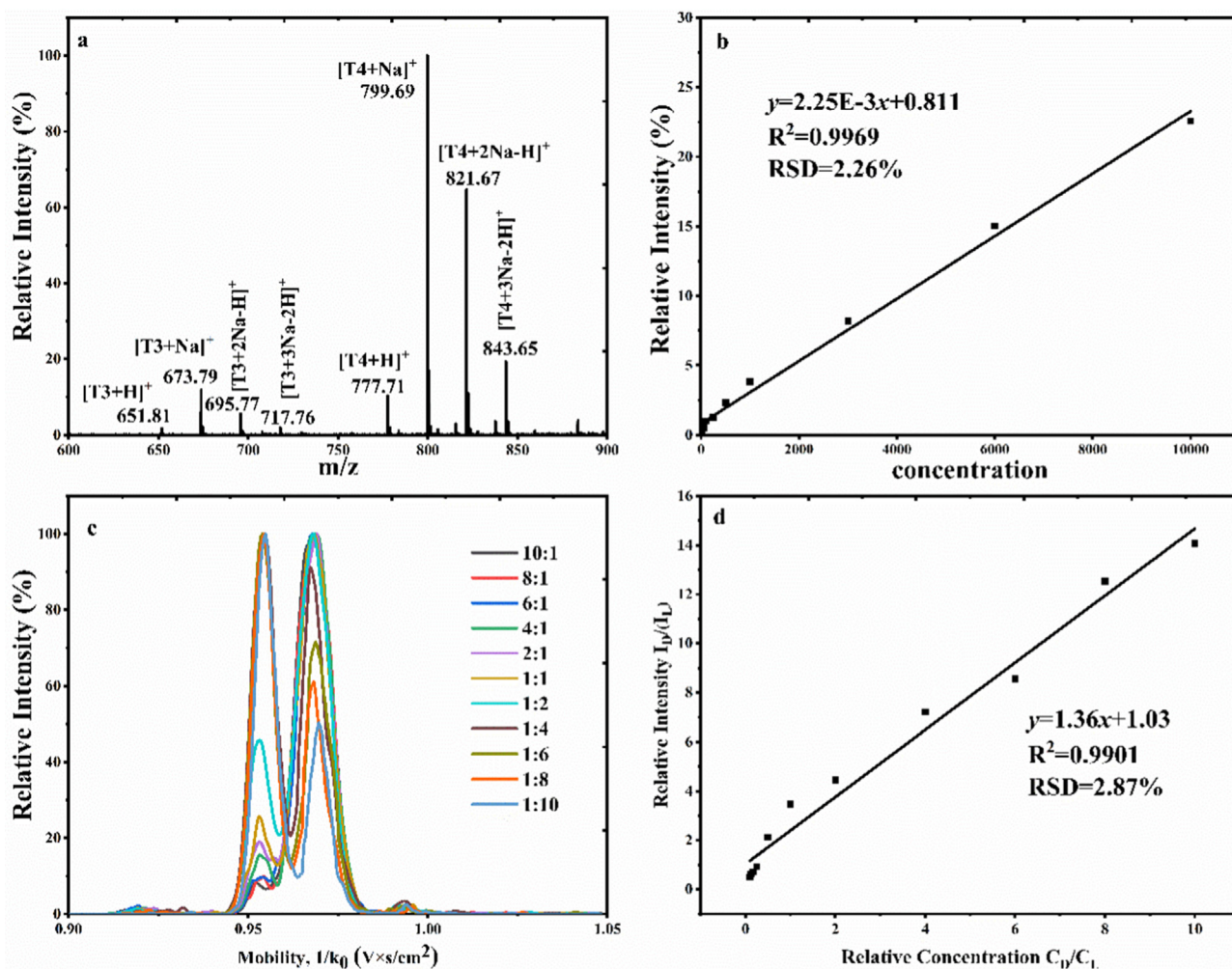


**Fig. 7** Absolute quantification using the T3 as the interior label (a) Mass spectra for the mixture TT (100.0 ng/mL) T4 (5000 ng/mL); (b) standard curve; Relative quantification for the D/L-T4 enantiomers (c) extracted ion mobility D: L = 10:1–1:10; (d) standard curve.



**Table 2** Quality control measured for the proposed method.

Absolute quantification			
	High (ng mL <sup>-1</sup> )	Medium (ng mL <sup>-1</sup> )	Low (ng mL <sup>-1</sup> )
Spiked	9000.0	500.0	3.0
Detected	9000.0 ± 300.59	500.0 ± 10.27	3.0 ± 0.11
RSD%	3.33%	2.05%	3.67%
Relative quantification			
	High (molar ratio)	Medium (molar ratio)	Low (molar ratio)
Spiked	10:3	10:9	1:9
Detected	10 ± 0.66:3 ± 0.20	10 ± 0.75:9 ± 0.64	1 ± 0.11:9 ± 0.77
RSD%	5.67%	5.61%	4.67%

### 3.6. Detection of D/L-T4 enantiomers in practical samples

The proposed method for D/L-T4 detection in practical sample of drug tablets as example for method validation. Firstly, the total T4 content (including D-T4 and L-T4) was detected by using L-T3 as the internal standard. And the content of the T4 was back calculated by the absolute quantitative standard curve in Fig. 7b via their mass peak intensity. Accordingly, T4 detected in the tablets was 45.3–52.6 ug with the RSD ≤ 4.65%, which was basically the same as the amount described in the manual. Moreover, the sample was further mobility separating to determine whether L-T4 contains D-T4 in the tablets. The TIMS-MS results was shown that the D-T4 was basically undetectable in the drug tablets, revealed this drug tablets with better purity.

Additional, 5.0 ug D-T4 was added in the tablet, and TIMS-MS detected by complexing with β-CD and Ca<sup>2+</sup> in a diluted concentration of 10<sup>-6</sup> mol L<sup>-1</sup>. The detected molar ratios of D-T4 and L-T4 were back calculated by the measured relative quantitative standard curves, the detected molar concentration ratio was 1.0 ± 0.32:10.0 ± 0.54 for the D-T4:L-T4. These results reveal that the proposed method can be applied to D/L-T4 enantiomer analysis and take the fake test in practical samples.

## 4. Conclusion

In this work, chiral enantiomer of D/L-T4 was separated and quantified by TIMS-MS through simply mixing with CD and metal ions. By simply mixing with CDs, a certain degree of separation of D/L-T4 was obtained by the form binary diastereomeric complexes, which the separation effect for D/L-T4 in a following of α-CD ( $R_{p-p} = 0.411$ ) > β-CD ( $R_{p-p} = 0.235$ ) > γ-CD ( $R_{p-p} = 0.118$ ). With the addition of divalent metal ions, the related bivalent ternary diastereomer complexes can be formed, and the separation effect was improved to 1.59 ( $R_{p-p}$ ) for D/L-T4 enantiomers by [α-CD + D/L-T4 + Ni]<sup>2+</sup>. Considering the D/L-T4 can be satisfactory separated by [β-CD + D/L-T4 + Ca]<sup>2+</sup> ( $R_{p-p} = 0.764$ ), and the high selectivity, non-toxic, chemically stable of β-CD, [β-CD + D/L-T4 + Ca]<sup>2+</sup> was selected for further D/L-T4 analysis. Moreover, chemical theoretical conformations for [β-CD + D/L-T4 + H]<sup>+</sup> and [β-CD + D/L-T4 + Ca]<sup>2+</sup> were optimized, discovering similar micro-interaction modes between [β-CD + D-T4 + H]<sup>+</sup> and [β-CD + L-T4 + H]<sup>+</sup>; and with the addition of Ca<sup>2+</sup>, significantly different interaction modes were observed between [β-CD + D-T4 + Ca]<sup>2+</sup> and [β-CD + L-T4 + Ca]<sup>2+</sup>. And theoret-

ical collision cross section (CCS) trends for the complexes were consistent with that of the experimental results. Additionally, quantitative analysis for D/L-T4 enantiomers was measured by [β-CD + D/L-T4 + Ca]<sup>2+</sup>. Good linear of R<sup>2</sup> higher than 0.99 and high accuracy RSD ≤ 2.87% were obtained, with LOD for T4 analysis was 0.11 ng mL<sup>-1</sup>, and detection scope for D/L-T4 was in the scop range of 45.6:1 to 1:59.8. Finally, the method was successfully applied to the D/L-T4 analysis in drug tablet, revealing the proposed method possesses the advantages of simplicity, selectivity, speed (<5 min), and lack of chemical derivation or chromatographic separation, that can be an effective approach for D/L-T4 analysis or even other thyroxine isomers in practical samples.

## Acknowledgment

This work was supported by Zhejiang Natural Science Foundation (LY22B050006), National Natural Science Foundation of China (22004074 and 21927805), and the Science and Technique Plans of Ningbo City (2019C50080).

## Conflict of interest

All the authors declare no conflict of interest.

## Appendix A. Supplementary data

Supplementary data to this article can be found online at <https://doi.org/10.1016/j.arabjc.2023.104718>.

## References

- An, Q., Wang, L., Ding, X.Y., Shen, Y.J., Hao, S.H., Li, W.J., Zhang, D., 2022. Validation of Sennae Folium specification grade classification based on UPLC-Q-TOF/MS spectrum-effect relationship. *Arab. J. Chem.* 15, (11) 104223.
- Bai, H., Wang, J., Phan, C.U., Chen, Q., Hu, X., Shao, G., Tang, G., 2021. Cyclodextrin-based host-guest complexes loaded with regorafenib for colorectal cancer treatment. *Nat. Commun.* 12, 1–18.
- Bowerbank, S.L., Carlin, M.G., Dean, J.R., 2019. A direct comparison of liquid chromatography-mass spectrometry with clinical routine testing immunoassay methods for the detection and quantification of thyroid hormones in blood serum. *Anal. Bioanal. Chem.* 411, 2839–2853.
- Campuzano, I., Bush, M.F., Robinson, C.V., Beaumont, C., Richardson, K., Kim, H., Kim, H.I., 2012. Structural characterization of drug-like compounds by ion mobility mass spectrometry: comparison of theoretical and experimentally derived nitrogen collision cross sections. *Anal. Chem.* 84 (2), 1026–1033.
- Cerit, Z., 2017. Epicardial Adipose Tissue, Carotid Intima-Media Thickness, and Thyroid Disorders. *Iran. J. Pediatr.* 27.
- Cumeras, R., Figueras, E., Davis, C.E., Baumbach, J.I., Gracia, I., 2015. Review on ion mobility spectrometry. Part I: current instrumentation. *Analyst* 140 (5), 1376–1390.
- Ding, Y., Cui, W., Pang, Y., Prasad, C.V.V., Wang, B., 2021. Preparation of inclusion complex of praziquantel with 2-hydroxypropyl-β-cyclodextrin and pharmacokinetic property improvement. *Arab. J. Chem.* 14, (9) 103307.
- Dodds, J.N., Baker, E.S., 2019. Ion mobility spectrometry: fundamental concepts, instrumentation, applications, and the road ahead. *J. Am. Soc. Mass. Spectrom.* 30, 2185–2195.
- Dogan, A., Plotka-Wasylik, J., Kempńska-Kupczyk, D., Namieśnik, J., Kot-Wasik, A., 2020. Detection, identification and determination of chiral pharmaceutical residues in wastewater: Problems and challenges. *TrAC Trend Anal. Chem.* 122, 115710.

- Eberhardt, J., Santos-Martins, D., Tillack, A.F., Forli, S., 2021. AutoDock Vina 1.2. 0: New docking methods, expanded force field, and python bindings. *J Chem. Inf. Model.* 61 (8), 3891–3898.
- Fernandez-Lima, F.A., Kaplan, D.A., Park, M.A., 2011. Note: Integration of trapped ion mobility spectrometry with mass spectrometry. *Rev. Sci. Instrum.* 82, 126106.
- Fouque, K.J.D., Fernandez-Lima, F., 2019. Recent advances in biological separations using trapped ion mobility spectrometry–mass spectrometry. *TrAC-Trend Anal. Chem.* 116, 308–315.
- Griffiths, J., 2018. A brief history of mass spectrometry. *Anal Chem* 80, 5678–5683.
- Han, D.Q., Yao, Z.P., 2020. Chiral mass spectrometry: an overview. *TrAC-Trend Anal. Chem.* 123, 115763.
- Jin, D., Kumar, A.P., Song, G.C., Lee, Y.I., 2008. Determination of thyroxine enantiomers in pharmaceutical formulation by high-performance liquid chromatography–mass spectrometry with pre-column derivatization. *Microchem. J.* 88, 62–66.
- Liu, Y., Chen, Y., Gao, X., Fu, J., Hu, L., 2022a. Application of cyclodextrin in food industry. *Crit Rev Food Sci Nutr* 62, 2627–2640.
- Liu, C., Deng, Q., Fang, G., Dang, M., Wang, S., 2017. Capillary electrochromatography immunoassay for alpha-fetoprotein based on poly (guanidinium ionic liquid) monolithic material. *Anal. Biochem.* 530, 50–56.
- Liu, Y., Wu, F., Wang, J., Pu, L., Ding, C.F., 2022b. Simultaneous chirality separation of amino acids and their derivative by natamycin based on mobility measurements. *Anal. Chim. Acta* 1227, 340298.
- Luongo, C., Dentice, M., Salvatore, D., 2019. Deiodinases and their intricate role in thyroid hormone homeostasis. *Nat. Rev. Endocrinol.* 15, 479–488.
- Mourouzis, I., Forini, F., Pantos, C., Iervasi, G., 2011. Thyroid hormone and cardiac disease: from basic concepts to clinical application. *J Thyroid. Res.* 958626, 13.
- Olajide, O.E., Donkor, B., Hamid, A.M., 2021. Systematic optimization of ambient ionization ion mobility mass spectrometry for rapid separation of isomers. *J Am. Soc. Mass Spectr.* 33 (1), 160–171.
- Putri, A.R., Aliaño-González, M.J., Ferreira, M., Setyaningsih, W., Rohman, A., Riyanto, S., Palma, M., 2020. Development of a methodology based on headspace-gas chromatography-ion mobility spectrometry for the rapid detection and determination of patin fish oil adulterated with palm oil. *Arab. J. Chem.* 13 (10), 7524–7532.
- Razvi, S., Jabbar, A., Pingitore, A., Danzi, S., Biondi, B., Klein, I., Iervasi, G., 2018. Thyroid hormones and cardiovascular function and diseases. 71, 1781–1796.
- Shrivastav, V., Nahin, M., Hogan, C.J., Larriba-Andaluz, C., 2017. Benchmark comparison for a multi-processing ion mobility calculator in the free molecular regime. *J Am. Soc. Mass Spectr.* 28, 1540–1551.
- Taira, S., Shikano, H., Takahashi, N., 2022. Analysis of hair components by nanoparticle-assisted laser desorption/ionization mass spectrometry imaging. *Arab. J. Chem.* 15, (11) 104205.
- Weedbrook, C., Pirandola, S., García-Patrón, R., Cerf, N.J., Ralph, T. C., Shapiro, J.H., Lloyd, S., 2012. Gaussian quantum information. *Rev. Mod. Phys.* 84 (2), 621.
- Woo, N., Kim, S.K., Kang, S.H., 2017. Multi-immunoreaction-based dual-color capillary electrophoresis for enhanced diagnostic reliability of thyroid gland disease. *J. Chromatogr. A.* 1509, 153–162.
- Wu, X., Li, W., Li, C., Yin, J., Wu, T., Zhang, M., Li, Z., 2022c. Discrimination and characterization of the volatile organic compounds of *Acori tatarinowii* rhizoma based on headspace-gas chromatography-ion mobility spectrometry and headspace solid phase microextraction-gas chromatography-mass spectrometry. *Arab. J. Chem.* 15, (11) 104231.
- Wu, F., Yang, S., Dai, X., Gu, L., Tang, K., Xu, F., Ding, C.F., 2021. A simple strategy for dl malic acid recognition and quantification using trapped ion mobility spectrometry. *Microchem. J.* 16, 106301.
- Wu, F., Wu, X., Chi, C., Ding, C.F., 2022a. Simultaneous Differentiation of C=C Position Isomerism in Fatty Acids through Ion Mobility and Theoretical Calculations. *Anal. Chem.* 94, 12213–12220.
- Wu, F., Wu, X., Li, Z., Zhang, D., Ding, C.F., 2022b. A Cyclodextrin-Based Reagent for Cis/Trans-Geometrical Isomers Separation by Mobility Measurements and Chemical Calculations. *Food Chem.* 135027.
- Xiao, W., Yang, Z., Liu, J., Chen, Z., Li, H., 2022. Sensitive cholesterol determination by  $\beta$ -cyclodextrin recognition based on fluorescence enhancement of gold nanoclusters. *Microchem. J.* 175, 107125.
- Yu, X., Yao, Z.P., 2017. Chiral recognition and determination of enantiomeric excess by mass spectrometry: A review. *Anal. Chim. Acta* 968, 1–20.